

INVESTIGATION INTO LASER REFINISHMENT AND TRANSFORMATION HARDENING OF CAST IRON FORMING DIES FOR THE AUTOMOTIVE INDUSTRY

Paper #258

Maritha Theron¹, Corney van Rooyen¹, Khoro Malabi¹

¹National Laser Centre, Council for Scientific and Industrial Research, Pretoria, 0001, South-Africa

Abstract

Forming dies used in the automotive industry are shaped as such that it imparts a predetermined contour or profile to the workpiece. Due to the subsequent assembly requirements of sheet-formed body structure components, the dimensional accuracy of the components is of vital importance. The dimensional accuracy of the forming dies is therefore of equal importance. The sheet metal forming process involves severe contact conditions, with the draw die radius generally being the most affected zone. Due to intense local tribological conditions, wear damage is observed.

The possible laser refurbishment of wear damaged cast iron die radii has been investigated as well as laser transformation hardening of these areas. The refurbishment is seen as a remedy to an existing problem and the transformation hardening as a precautionary wear-inhibiting solution to the problem. Due to the high carbon content of the cast iron and the dilution - although low - obtained during the cladding process, the resulting build-up susceptibility to cracking can be high. A stainless steel buffer layer between the die substrate and the overlay material was introduced. It was found that the H11 overlay material hardness complied with the specific requirement.

The laser transformation hardening was studied at different parameter sets to obtain the required surface hardness and the laser hardening was successfully implemented on a forming die which was put in service.

Introduction

Metal forming is critical to industrial operations supplying automotive parts and a stamping / punching tool or forming die must be replaced or repaired periodically. This is required when the tool or die fails to produce parts within the specified tolerance and / or required surface quality, because the automobile market demands high precision and perfect quality [1]. The wear on a punch or die will vary greatly depending on the type of metal being formed and the

amount of pressure exerted on it, whereas the wear mechanisms are depending on tool material, surface finish and coating properties [2].

Considering the high cost of coated tool steels, large forming tools are generally made of relatively inexpensive and soft materials, such as cast iron or low-grade tool steel. This results in high wear rates of the forming tools in specific areas during operation, due to severe contact conditions. The zone that is most affected by wear damage, is the die radius and the wear is resulting from severe local interaction of surfaces in relative motion. Other damage that can occur includes chipping and surface cracking [2,3,4].

The decision to either repair or replace a damaged tool mainly depends on the cost of each and the expected tool life of either selection. If tool refurbishment is opted for, welding is the only technology suitable and there are different welding processes available for the refurbishment. In order to achieve a sound weld repair, factors like heat treatment and proper filler material should be considered. Arc welding is widely used and normally gas tungsten arc welding is chosen due to its flexibility, accuracy and energy concentration. Laser welding is however the newer process used for refurbishment, due to its accuracy, the limited machining required after the repair as a result of the controlled deposition rate and limited influence that the laser weld bead has on the substrate [4,5].

Experimental

The experimental trials were done on GGG70 cast iron (composition specification given in Table 1) which was the same for the forming die to be heat treated. The study included laser cladding as well as laser transformation hardening as remedial and wear-inhibiting solutions respectively.

Table 1 Chemical composition specification for the GGG70 base material (wt%) [6]

	C	Mn	Si	S	P	Bal.
GGG	3.25	0.10	2.4	0.005	0.015	Fe
70	3.70	0.30	3.0	0.020	0.080	

A fibre-coupled Rofin Sinar DY044 Nd:YAG laser was utilised in these experiments for both the deposition of clad tracks onto the substrate and the hardening. The laser was coupled to a 6-axes KUKA KR60L articulated arm robot which controlled the movement.

Laser Transformation Hardening

A Mergenthaler fibre-coupled infrared pyrometer system for temperature measurement together with a LASCON closed loop controller was attached to a Precitec YW50 laser head. The pilot light was aligned to coincide with the laser spot on the surface of the substrate. By setting the required temperature on the pyrometer system and measuring the actual surface temperature, the laser power could be controlled in such a way that the surface temperature and the corresponding hardening depth were maintained on the required level.

A small casting replica of the forming die, with the correct angled profile, was supplied for laser hardening trials, together with a smaller casting sample. The as-received material hardness averaged 22 HRC and the aim was to increase the designated area hardness (Figure 1) to a maximum, with a case depth as high as possible.

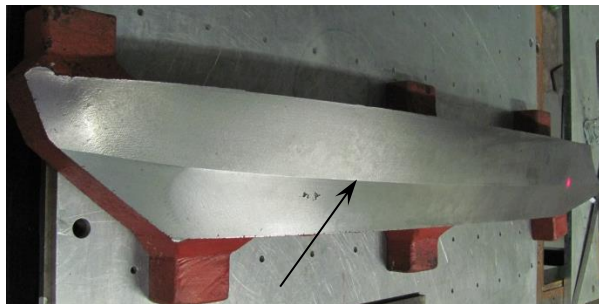


Figure 1 Small casting replica of the forming die that was supplied for laser hardening tests. The angled profile is indicated by the arrow
(Courtesy of Volkswagen Group South Africa)

The additional small casting sample was used for parameter window determination and analysis of the hardened tracks. An area was also machined to duplicate the angled profile of the replica. This was done to do trials with the angle of incidence of the laser beam in order to determine the least damage to the angled profile and most evenly hardened track.

The hardness of each track was measured by means of a TIME TH-134 portable hardness tester and the optimum set of parameters was determined. These parameters were used to laser harden the casting

sample before a representative transverse sample of the track was cut, mounted and polished for Vickers micro-hardness testing and microstructure analysis. A hardness traverse from the angle surface down into the base material was done to determine the case depth and a sub-surface hardness traverse was done to determine the obtained track width. A load of 300g was applied and a sub-surface traverse was done at a distance of 200 μ m from the surface.

These hardening parameters were then applied onto the punch die replica to confirm the obtained hardness and track width. Finally the same parameters were used to harden the forming die.

Laser Cladding

The clad metal for repair was initially only H11 tool steel powder, but due to very poor clad integrity, a low carbon martensitic stainless steel powder (1.7339) was included into the study. The stainless steel metal was applied as buffer material and the H11 as overlay material. The powder particles were spherical with a size range between 45 and 90 μ m. The chemical composition for these two metal powders is given in Table 2. It was carried to the workpiece by means of a GTV powder feeder together with an ILT three-way cladding nozzle.

Table 2 Chemical composition for the two clad metal powders

	C	Mn	Si	Cr	Mo	V	Bal.
1.7339	0.1	1.0	0.6	1.0	0.5	-	Fe
H11	0.35	0.3	0.95	5.1	1.3	0.45	Fe

Both a 2 mm and 4 mm spot diameter were used during the repair process experiments. The laser power was varied between 1 kW and 1.8 kW for the 2 mm diameter spot, while it ranged from 1.8 kW to 3 kW for the 4 mm diameter spot. The travel speed was varied between 0.6 and 1.2 m/min and argon was used as shielding and carrier gas.

Different combinations of single and multiple layers of each material were cladded onto mild steel substrate as well as the GGG70 substrate (casting sample as well as the casting replica). The hardness of the clad on the replica was again measured by means of the portable hardness tester, since the replica could not be cut.

The standard 50 % overlap between clad tracks was mainly applied, but higher and lower percentages have also been studied, together with the effect of a cool-down period between the buffer layer and overlay, as well as the different overlay layers.

Results and Discussion

Laser Transformation Hardening

The optimal hardening parameter track done on the machined cast sample, is shown in Figure 2. The transverse micrograph of this hardened track is shown in Figure 3 and the measured hardness traverses for it are shown in Figure 4.

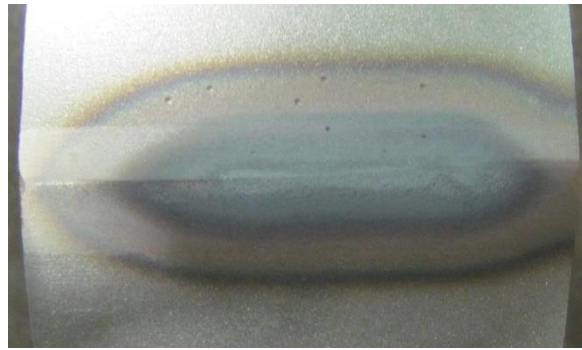


Figure 2 Typical appearance of the machined casting sample with the optimal hardening parameter track

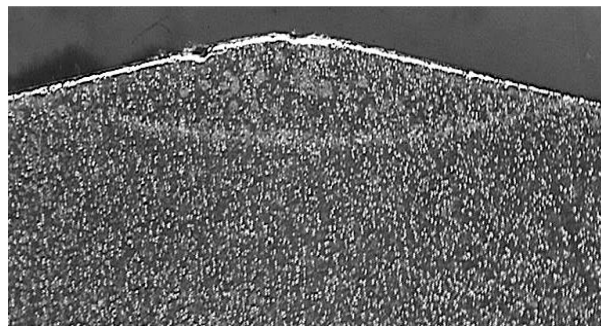


Figure 3 Transverse micrograph of the laser hardened track, showing the case depth as well as the track width

From Figure 4(a) it can be seen that the case depth obtained on the cast sample when laser hardened with the optimum parameters, was in the order of 2.3mm, when the minimum required hardness is taken as 500 HV (49 HRC). Attention should however be brought to the fact that the case depth decreases with increasing distance from the centre of the angled profile, due to the geometry of the case (Figure 3).

Figure 4(b) shows that the effective hardened track width (taken with 500 HV as minimum required hardness) is typically 10 mm (5 mm each side from the centre of the angle). This width also increases as the minimum required hardness decreases. The visible hardened width measured on the surface was therefore 14 mm, but the total hardening track width was about 28 mm (heat affected zone (HAZ) included).

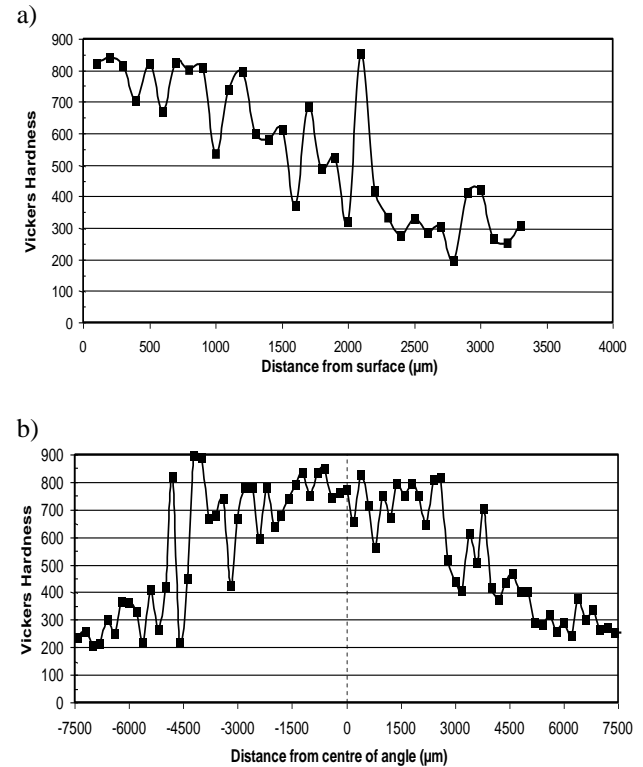


Figure 4 Vickers hardness traverse of the optimally hardened cast sample track from the surface into the base material (a) and sub-surface (200 μ m below surface) (b)

These laser hardening parameters were then applied to the punch die replica which had a coarser surface finish than the cast sample. The obtained hardened track is shown in Figure 5, together with the average Rockwell C hardness measured with the portable, handheld hardness tester in different positions. The case depth obtained on this replica could not be determined since it could not be cut for analysis. The effectively hardened track width on the surface was again measured as 14mm (7mm on each side from the centre of the angled profile), if 40.8 HRC (400 HV) is taken as the minimum required hardness.

The maximum hardness measured with the handheld hardness tester (equivalent to 530 HV) is much lower than that measured with the micro-hardness tester. This was probably because it was not possible to measure very close to the angle, which is the area of highest hardness, and the surface finish was much coarser than that of the polished sample. The accuracy of the measurement is also reliant on the perpendicular positioning of the tester onto the surface being tested.

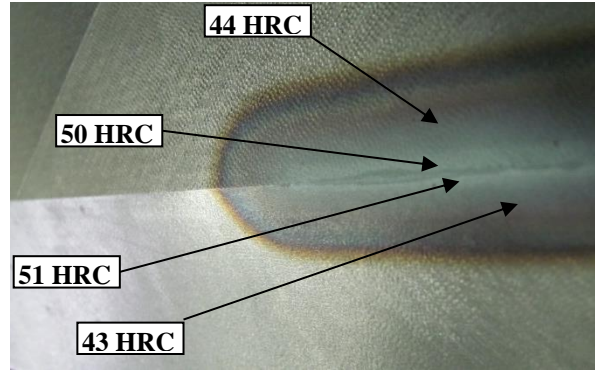


Figure 5 Laser hardening track obtained on the punch die replica, with the average measured Rockwell C hardness indicated on the different areas

All these trials were done beforehand and the same parameters used on the die replica, was used to harden the Volkswagen forming die. These parameters are given in Table 3. The full 4.4 kW laser power was required to reach the set temperature of 990 °C with the 0.2 m/min travel speed.

Table 3 Parameters selected for the laser transformation hardening done on the forming die

Pyrometer set temperature [°C]	Traveling speed [m/min]	Spot size [mm]
990	0.20	25 mm

The as-received angled profile of the forming die is shown in Figure 6 while the hardened profile is shown in Figure 7. From the close-up pictures it can clearly be seen that the forming line was hardened effectively and no damage was caused to it during the hardening process. The complete hardened track width again measured 30 mm and the effective hardened track width 14 mm. The hardness at the centre of the track was measured at the end of the hardening track (off the forming line) and registered 53 HRC.

Laser Cladding

The trials were started with the cladding of only H11 tool steel directly onto the GGG70 cast iron (Figure 8(a)). A transverse sample was cut from the area, mounted and polished for microstructural analysis. The result is shown in Figure 8(b). The average hardness of the H11 clad was measured to be 56 HRC and solidification cracking could clearly be detected both visually and microscopically.

Solidification cracks only occur in the weld metal and normally appear along the weld centreline, but may occasionally feature as transverse cracking. The latter

was the case with the H11 tool steel clad. The cracks were also visible on the surface (Figure 8), which is another characteristic of solidification cracking [7].



Figure 6 Part of the as-received forming die (a) with a close-up of the angled profile (b) (Courtesy of Volkswagen Group South Africa)



Figure 7 Part of the hardened forming die (a) with a close-up of the hardened angled profile (b)

The cracking was thought to be attributed to the dilution of impurities into the clad material, and a buffer layer between the cast iron and H11 was introduced. The low-C martensitic steel was used and the clad repair patch is shown in Figure 9, together with the cross section and microstructure.

This is the author's peer reviewed, accepted manuscript. However, the online version of record will be different from this version once it has been copyedited and typeset.
PLEASE CITE THIS ARTICLE AS DOI: 10.2351/7.0000106

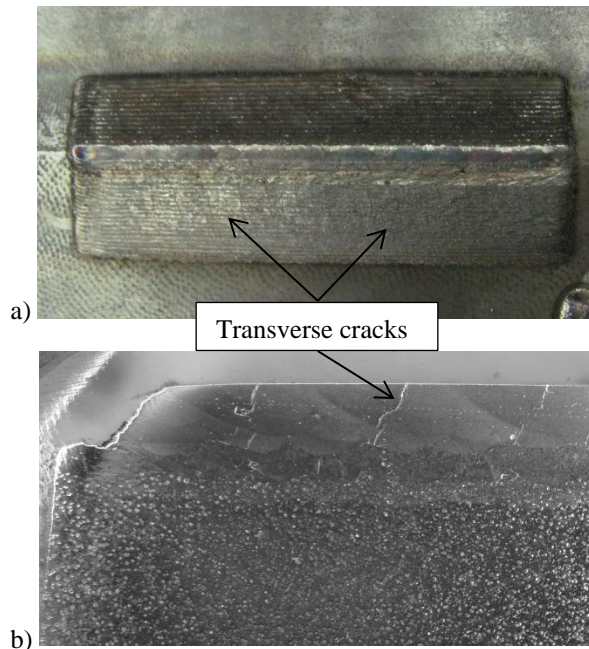


Figure 8 (a) H11 tool steel clad onto GGG70 cast iron with the angled profile, (b) Transverse micrograph of the clad

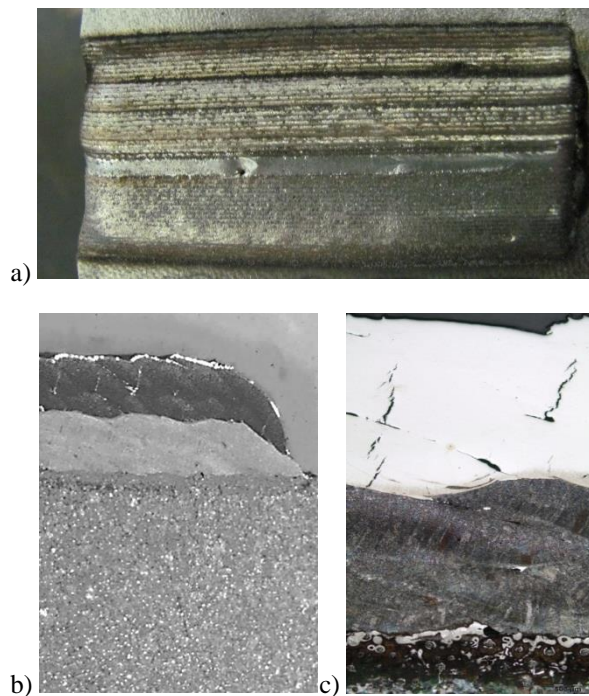


Figure 9 (a) Clad patch of the stainless steel buffer layer and H11 overlay on the GGG70 cast iron, (b) transverse section thereof and (c) microstructure of the three different material layers

These results highlighted the fact that the solidification cracking was not due to dilution, since two buffer

layers were cladded and only the first laser clad layer is typically affected by dilution from the substrate.

The principle cause of solidification cracking is insufficient strength of the weld bead in the final stage of solidification to withstand the contraction stresses generated as the weld pool solidifies. Factors which increase the cracking risk include insufficient weld bead size or shape, welding under high restraint or a relatively large amount of shrinkage on solidification [7]. All of these risk factors were the same for both the weld clad scenarios. Since there was no additional weld restraint and a large number of shrinkage cavities could be detected within the H11 clad layer(s), different bead sizes and shapes were investigated. This was done by varying the laser spot size, the overlap percentage between the adjacent tracks and the H11 layer thickness. The effect of a cool-down period in between the H11 layers on the solidification shrinkage was another factor being investigated.

It was observed that the higher percentage overlap (up to 70%) between adjacent tracks, which resulted in much thicker layers than usual (0.6 mm up to 1.2 mm), did not solve the solidification cracking problem. This is in agreement with general welding literature stating that the narrow, deep penetration welds with a low width/depth ratio can be susceptible to solidification cracking [7,8]. The lower percentage overlap (below 40 %) resulted in lack of fusion between the tracks.

The larger spot size (4 mm diameter) was applied to clad 0.8 to 1.2 mm thick layers, while 0.25 to 0.6 mm thick layers were built with the 2 mm spot diameter. The width to depth ratio for these layers therefore ranged between 3 and 5 for the 4 mm spot and between 3 and 8 for the 2 mm spot. Even though a ratio of 5 is quite high, none of the clad beads with a width to depth ratio equal to or below 5 resulted in solidification crack-free clads. However, the H11 clad repair process done with a 2 mm spot diameter and a width to depth ratio of between 6 and 8, proved to be successful.

When comparing the heat input between the 2 mm and 4 mm spot diameters (0.05 – 0.18 and 0.09 - 0.3 kJ/mm respectively), the range of the two spot sizes overlapped, but no crack-free clads could be obtained with the 4 mm spot size.

The cool-down period between the buffer layer and overlay or the different overlay layers was found to have no effect on the solidification cracking.

The travel speed was varied between 0.6 and 1.2 m/min, with the latter speed found to be the optimum for the 2 mm spot.

The process parameters found to be successful in producing crack-free H11 clads are listed in Table 4 and the build-up is shown in Figure 10 Three-layer H11 tool steel clad processed with the optimum parameters: (a) Stitched micrograph showing the full clad build-up and (b) Detail microstructure highlighting the crack-free, 0.4 mm thick layers. The complete repair build-up with the low martensitic stainless steel buffer layer (2 layers) as well as the H11 overlay (2 layers) is shown in Figure 11. The microhardness of the H11 overlay was measured on this build-up and the average was 673 HV.

Table 4 The H11 tool steel parameters determined for laser repair of GGG70 cast iron

Laser power [kW]	Travel speed [m/min]	Spot diameter [mm]	Overlap [%]	Layer thickness [mm]
1.2 - 1.5	1.2	2	50	0.25 - 0.4

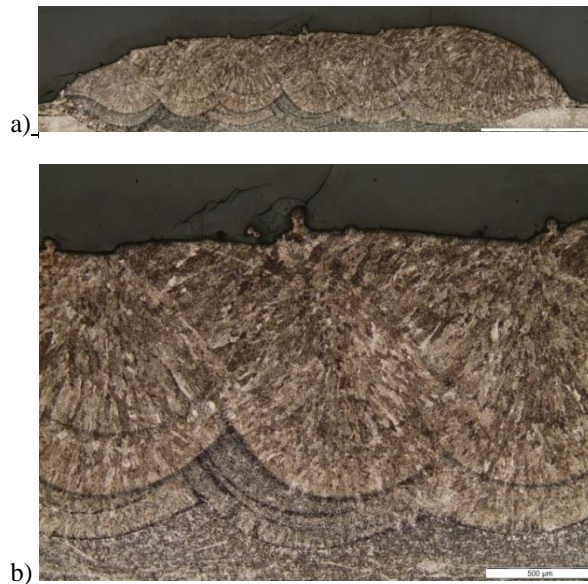


Figure 10 Three-layer H11 tool steel clad processed with the optimum parameters: (a) Stitched micrograph showing the full clad build-up and (b) Detail microstructure highlighting the crack-free, 0.4 mm thick layers

Conclusions

With regards to the laser transformation hardening of GGG70 cast iron components for the automotive industry, the following can be concluded:

- GGG70 cast iron can successfully be laser hardened up to an average surface hardness of 800 HV, a case depth of 2 mm and a case width of 12

mm with the laser system and optical configuration of the current study.

- The forming lines of a new stamping die could be laser hardened according to requirements, in order to inhibit wear of those areas. The die is still in use and has not required any maintenance on the forming lines.

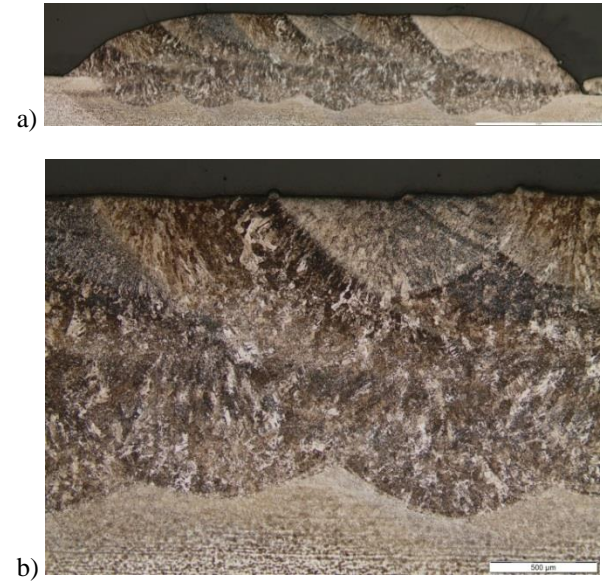


Figure 11 Complete clad repair build-up of the buffer layer together with the H11 overlay: (a) Stitched micrograph and (b) Detail microstructure

- Due to the very large heat sink of the forming die, the full power of the laser was required to reach the set temperature. An effective hardening track could therefore be obtained due to the self-quenching of the die.
- No damage was introduced to the angled profile of the forming lines during the hardening process.

The following can be concluded with regards to the clad repair of GGG70 cast iron components for the automotive industry:

- Solidification cracking within the H11 tool steel clad was the main area of concern for the clad repair process.
- Neither the increase in percentage overlap between adjacent tracks, which resulted in much thicker layers than usual, nor the bigger spot size solved the solidification cracking problem.
- The layer thickness, and therefore the width to depth ratio, proved to be the overriding factor in the successful cladding of a crack-free H11 build-up.

This is the author's peer reviewed, accepted manuscript. However, the online version of record will be different from this version once it has been copyedited and typeset.
PLEASE CITE THIS ARTICLE AS DOI: 10.2351/7.0000106

- The process parameters could be optimised in order to successfully produce crack-free H11 clads as well as complete repair build-ups with a buffer layer.

Acknowledgements

The authors would like to thank CSIR for funding the study and Volkswagen Group South Africa for providing the test samples.

References

- [1] Wang, X.Z., Masood, S.H. & Dingle, M.E. (2009) An investigation on tool wear prediction in automotive sheet metal stamping die using numerical simulation, in Proceedings of the International Multi-Conference of Engineers and Computer Scientists, Vol II, Hong Kong.
- [2] Attaf, D., Penazzi, L., Boher, C. & Levailant, C. (2002) Mechanical study of a sheet metal forming dies wear, in Proceedings of the 6th International Tooling Conference: The use of tool steels, Karlstad, Sweden, 179-190.
- [3] Hortig, D. & Schmoeckel, D. (2001) Analysis of local loads on the draw die profile with regard to wear using the FEM and experimental investigations, Journal of Materials Processing Technology 115(1), 153-158.
- [4] Tušek, J., Skumavc, A., Pompe, K. & Klobčar, D. (2014) Refurbishment of damaged tools using the combination of GTAW and laser beam welding, Metalurgija – Sisak then Zagreb 53(4), Ljubljana, 631-633.
- [5] Skszek, T. & Lowney, M.T.J. (2000) Die reconfiguration and restoration using laser-based deposition, Solid Freeform Fabrication Symposium, 219-226
- [6]<http://www.matweb.com/search/DataSheet.aspx?MatGUID=657fc4901905497ba441cb5a3b0a59db>
- [7]<https://www.twi-global.com/technical-knowledge/job-knowledge/defects-solidification-cracking-044>
- [8] Aucott, L.A. (2015) Mechanism of solidification cracking during welding of high strength steels for subsea pipeline, University of Leicester, Thesis.